

A MATHEMATICAL MODEL OF A FREQUENCY-CONTROLLED INDUCTION ELECTRIC DRIVE ON THE BASIS OF THE METHOD OF AVERAGE VOLTAGES IN INTEGRATION STEP

Mykola Semeniuk¹, Andriy Kutsyk¹, Vasyl Tutka²

¹ Department of Electromechanics and Computerized Electromechanical Systems,
Lviv Polytechnic National University, Ukraine

² PJSC Ivano-Frankivskcement, Ukraine

mykola.b.semeniuk@lpnu.ua, andrii.s.kutsyk@lpnu.ua

<https://doi.org/10.23939/jcpee2023.01>.

Abstract: Frequency-controlled electric drives are used in various industrial sectors due to the simplicity and reliability of the electric machine design, as well as the ability to provide the required control characteristics. This paper presents a mathematical model of a frequency-controlled electric drive with voltage source inverter developed by the Average Voltage in the Integration Step (AVIS) method and confirms its adequacy. A comparative analysis for the speed response and accuracy of the model calculation by the AVIS method, compared to known methods in Matlab/Simulink and to the known results of physical experiments, demonstrated the efficiency of using the AVIS method for modeling frequency-controlled induction electric drives in phase coordinates with taking into account the actual curves of currents, flux, and torque of electronically commutated induction machines.

Key words: variable frequency drive, induction motor, six-step inverter, AVIS method.

1. Introduction

Frequency-controlled electric drives are used in various industrial sectors, including increasing utilization in electric transportation, due to the simplicity and reliability of the electrical machine design and the ability to provide the necessary control characteristics of an electric drive as a whole [1-4]. In such an electric drive, an induction motor is powered by a voltage source inverter connected to a DC power source. Typically, a pulse-width modulation (PWM) inverter is used as the voltage source inverter. However, the disadvantage of such inverters is that the variable voltage is generated as a high-frequency sequence of pulses with different polarities. This leads to the occurrence of wave processes and, consequently, to overvoltages on the stator windings of the induction motor. In addition, the ripple nature of the voltage of a motor power supply causes a number of additional problems that reduce the motor service life, including voltage induction on the motor casing, current flow through the shaft and bearings leading to bearing damage, current leakage

through the power cable shields, accelerated aging of insulation, and electromagnetic emission [5]. An alternative solution to this problem is the use of three-phase voltage inverters with a different switching scheme, such as six-step voltage source inverters.

The objective of this research is to develop a mathematical model of a frequency-controlled induction electric drive using the AVIS method and to analyze the adequacy, accuracy, and computational speed of the response of the developed model compared to known numerical integration methods, taking into account the nonsinusoidal nature of the motor power supply.

For the synthesis of control systems, fast-response models are necessary, particularly, models in phase coordinates that can replicate the real curves of currents, flux, and torque in electronically commutated induction machines. The mathematical model of the frequency-controlled induction electric drive was developed using the AVIS method [6,7]. This method has demonstrated its effectiveness in modeling electrical power systems with synchronous machines and induction motors [7-10]. The advantages of the method include high computational speed of response and numerical stability, making it suitable for creating real-time models capable of operating for extended periods in interaction with physical objects (hardware-in-the-loop technology). This approach can serve as an alternative to well-known Matlab-based models, which, although being often used, tend to operate relatively slowly.

2. Mathematical model description

The universal equation for an electrical branch containing an active resistance R , inductance L , capacitance C and an additional electromotive force (emf) using the AVIS method is given by:

$$\left(\frac{R}{m+1} + \frac{\Delta t}{C} \cdot \frac{2-(m+1)(m+2)}{2(m+1)(m+2)} \right) i_0 + \frac{\Psi_0}{\Delta t} - u_{R0} - u_{C0} - \sum_{k=1}^{m-1} \left(\frac{R \Delta t^k}{(k+1)!} \cdot \frac{m-k}{m+1} \right) \frac{d^k i_0}{dt^k} -$$

$$-\sum_{k=1}^{m-1} \left(\frac{(m+1)(m+2) - (k+1)(k+2)\Delta t^{k+1}}{(m+1)(m+2)C(k+2)!} \right) \frac{d^k i_0}{dt^k} \quad (1)$$

$$+ U + E - \left(\frac{R}{m+1} + \frac{\Delta t}{C(m+1)(m+2)} \right) i_1 - \frac{\psi_1}{\Delta t} = 0.$$

where i_0 is the branch current at the beginning of the integration step; m is the order of the polynomial describing the current waveform at the integration step

$$(the\ order\ of\ the\ method); \quad U = \frac{1}{\Delta t} \int_{t_0}^{t_0+\Delta t} u dt, \quad E = \frac{1}{\Delta t} \int_{t_0}^{t_0+\Delta t} e dt$$

are average values of the applied voltage and electromotive force in the branch at the numerical integration step; u_{C0} is the voltage across the capacitor at the beginning of the numerical integration step; u_{R0} is the voltage across the active resistance at the beginning of the numerical integration step; ψ_0, ψ_1 are flux linkages at the beginning and at the end of the numerical integration step; Δt is the integration step.

From equation (1), for a branch without capacitance and an additional emf source, a formula for the AVIS method of 1st order is obtained:

$$U - u_{R0} + \frac{R}{2} i_0 - \frac{R}{2} i_1 + \frac{1}{\Delta t} (\psi_0 - \psi_1) = 0, \quad (2)$$

For the AVIS method of the 2nd order it will look like:

$$U - u_{R0} + \frac{R}{3} i_0 - \frac{R\Delta t}{6} \frac{di_0}{dt} - \frac{R}{3} i_1 + \frac{1}{\Delta t} (\psi_0 - \psi_1) = 0. \quad (3)$$

Equations (2) and (3) are the basis for developing the mathematical model of an induction motor (IM).

Mathematical model of electric circuits for IM using the AVIS method of 1st order

Basing on equation (2) and taking into account that the change in flux linkages at the integration step is determined as $\Delta \vec{\psi}_{am} = L_{am1} \vec{i}_1 - L_{am0} \vec{i}_0$, the vector equation for the stator and rotor windings is determined by the following formula:

$$\vec{U} - \mathbf{R} \vec{i}_0 + \left(\frac{\mathbf{R}}{2} + \frac{\mathbf{L}_{am0}}{\Delta t} \right) \vec{i}_0 - \left(\frac{\mathbf{R}}{2} + \frac{\mathbf{L}_{am1}}{\Delta t} \right) \vec{i}_1 = 0, \quad (4)$$

where $U = \frac{1}{\Delta t} \int_{t_0}^{t_0+\Delta t} u_{am}(t) dt$ is the vector of average

voltages at the integration step;

$$\mathbf{u}_{am} = (u_A, u_B, u_C, u_a, u_b, u_c)^T = (u_A, u_B, u_C, 0, 0, 0)^T$$

are instantaneous values of voltages of the stator and squirrel cage rotor;

$$\vec{i}_0 = (i_{A0}, i_{B0}, i_{C0}, i_{a0}, i_{b0}, i_{c0})^T$$

$$\vec{i}_1 = (i_{A1}, i_{B1}, i_{C1}, i_{a1}, i_{b1}, i_{c1})^T$$

are the vectors of currents at the beginning and at the end of the integration step;

$$\mathbf{R}_{am} = \text{diag}(R_A, R_B, R_C, R_a, R_b, R_c)$$

is the matrix of active resistances; $\mathbf{L}_{am0} = \mathbf{L}_{am}(\gamma_{R0})$, $\mathbf{L}_{am1} = \mathbf{L}_{am}(\gamma_{R1})$ are matrices of inductances at the beginning and at the end of the integration step, which are functions of the rotor angle, γ_{R0}, γ_{R1} is the rotor angle at the beginning and the end of the integration step.

Based on equation (4), the equivalent circuit of the IM is represented as shown in Fig. 1.

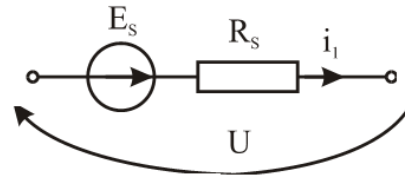


Fig. 1. The equivalent circuit of the IM.

Fig. 1 depicts the following:

$$\vec{E}_s = \mathbf{R} \vec{i}_0 - \left(\frac{\mathbf{R}}{2} + \frac{\mathbf{L}_{am0}}{\Delta t} \right) \vec{i}_0 = \left(\frac{\mathbf{L}_{am0}}{\Delta t} + \frac{\mathbf{R}}{2} \right) \vec{i}_0$$

is the step e.m.f. (which is determined by the values of currents and electromagnetic parameters at the beginning of the integration step), $\mathbf{R}_s = \left(\frac{\mathbf{R}}{2} + \frac{\mathbf{L}_{am1}}{\Delta t} \right)$ is the step resistance.

According to the equivalent circuit, the vector of currents in the electrical machine (AM) at the end of the step is determined by the following equation:

$$\vec{i}_1 = \frac{\vec{U} + \vec{E}_s}{\mathbf{R}_s}, \quad (5)$$

Mathematical model of electric circuits for the IM using the AVIS method of 2nd order

Basing on equation (3) and taking into account that the change in flux linkages at the integration step is determined as $\Delta \vec{\psi}_{am} = L_{am1} \vec{i}_1 - L_{am0} \vec{i}_0$, the vector equation for the stator and rotor windings is obtained as follows:

$$\vec{U} - \mathbf{R} \vec{i}_0 + \left(\frac{\mathbf{R}}{3} + \frac{\mathbf{L}_{am0}}{\Delta t} \right) \vec{i}_0 - \frac{R\Delta t}{6} \frac{d\vec{i}_0}{dt} - \left(\frac{\mathbf{R}}{3} + \frac{\mathbf{L}_{am1}}{\Delta t} \right) \vec{i}_1 = 0. \quad (6)$$

The parameters of the equivalent circuit (Fig. 1) in this case will be determined as follows:

$$\vec{E}_s = \left(\frac{\mathbf{L}_{am0}}{\Delta t} - \frac{2\mathbf{R}}{3} \right) \vec{i}_0 - \frac{R\Delta t}{6} \frac{d\vec{i}_0}{dt}$$

is the step e.m.f. (which is determined by the values of currents and electromagnetic parameters at the beginning of the integration step), $\mathbf{R}_s = \left(\frac{\mathbf{R}}{3} + \frac{\mathbf{L}_{am1}}{\Delta t} \right)$ is the step resistance.

The vector of IM currents at the end of the step is determined according to formula (5).

To determine the currents of the IM windings using the 2nd order AVIS method, the derivatives of the currents are used (as they are involved in the expression of the step electromotive force). These derivatives are found according to the following equation:

$$\bar{U} = \mathbf{R}\bar{i} + \frac{d\bar{\psi}_{am}(\bar{i}, \gamma_R)}{dt}, \quad (7)$$

Taking into account that the flux linkage in equation (7) is a function of currents and the rotor angle, their derivatives will be determined as follows:

$$\frac{d\bar{\psi}_{am}(\bar{i}, \gamma_R)}{dt} = \mathbf{L}_{am} \frac{d\bar{i}}{dt} + \frac{\partial \mathbf{L}_{am}}{\partial \gamma_R} \bar{i} z_p \omega_R = \bar{E}_{TR} + \bar{E}_{ROT}, \quad (8)$$

where z_p is the number of pole pairs, ω_R is rotor angular velocity, $\bar{E}_{TR}, \bar{E}_{ROT}$ are transformer EMF and rotational EMF (components of stator EMF).

From equations (7) and (8), the expression for determining the derivatives of the currents is derived:

$$\frac{d\bar{i}}{dt} = \left(\bar{U} - \mathbf{R}\bar{i} - \frac{\partial \mathbf{L}_{am}}{\partial \gamma_R} \bar{i} z_p \omega_R \right) \mathbf{L}_{am}^{-1}.$$

The rotor angle and rotational speed are determined from equations describing the mechanical part of the IM:

$$\frac{d\gamma_R}{dt} = z_p \omega_R, \quad (9)$$

$$\frac{d\omega_R}{dt} = \frac{M_{am} - M_L}{J}, \quad (10)$$

where M_{am} is the electromagnetic torque of the IM; M_L is the load torque; J is the moment of inertia.

The voltage source inverter in the model is described by the conductivity functions of the respective phases g_a, g_b, g_c , which take values of 1 and -1. In this case, the output voltage of the inverter is determined by the formula:

$$u_A = g_A(t) \frac{U_{DC}}{2} - V_0, u_B = g_B(t) \frac{U_{DC}}{2} - V_0, \quad (11)$$

$$u_C = g_C(t) \frac{U_{DC}}{2} - V_0,$$

where U_{DC} is the input voltage of the inverter, V_0 is the potential of a zero point.

The input current of the voltage source inverter is determined as follows:

$$I_{DC} = \frac{1}{2}(g_A(t)i_A + g_B(t)i_B + g_C(t)i_C), \quad (12)$$

In the case of using a six-step voltage source inverter to supply an IM drive, the conduction functions g_a, g_b, g_c for each phase are determined as follows. If $0 < \omega t < \pi$, the conduction function for phase A is 1; otherwise, it is -1. If $\frac{2\pi}{3} < \omega t < \frac{5\pi}{3}$, the conduction

function for phase B is 1; otherwise, it is -1. If $\frac{4\pi}{3} < \omega t < 2\pi$ and $0 < \omega t < \frac{\pi}{3}$, the conduction function for phase C is 1; otherwise, it is -1.

In the case of using a PWM voltage source inverter to supply the IM drive, the triangle carrier wave with a frequency of 10 kHz is compared with the modulation wave for each phase, which can be expressed by the following formulas:

$$U_{ka} = U_m \sin(\omega t),$$

$$U_{kb} = U_m \sin(\omega t - \rho), \quad (13)$$

$$U_{kc} = U_m \sin(\omega t + \rho),$$

where U_m is a peak value of the modulation wave, $\rho = \frac{2\pi}{3}$, $\omega = 2\pi f$ is the angular frequency of the voltage at the output of the inverter.

In the case when the modulation voltage for phase A is greater than the triangle carrier voltage, the conduction function for phase A is 1; otherwise, it is -1. Similarly, the conductivity functions for phases B and C are determined on the basis of a similar comparison between the modulation voltages and the triangle carrier voltage.

To simulate the frequency startup of the IM drive, the frequency of the stator voltage f_s is varied according to a linear law. In this case, the input voltage of the inverter U_s is determined according to the following expression:

$$U_s = \frac{(U_n - U_{min})}{(f_n - f_{min})} f_s \quad (14)$$

where U_n, f_n are the nominal stator voltage and nominal frequency of the IM, respectively; U_{min}, f_{min} are the minimum stator voltage and minimum frequency of the IM.

3. Simulation results

The evaluation of the efficiency of the AVIS method was carried out via comparative analysis of the simulation results using the AVIS method and other well-known numerical integration methods implemented with standard Matlab/Simulink functions. The comparison was conducted for the frequency startup of the induction motor, which is characterized by a significant range of coordinate variations. The parameters of the IM used during the simulation were as follows: type 2SIE315S2, $P_N=110$ kW, $U_N=380$ V, $I_N=192$ A, $L_{\sigma 1}=L'_{\sigma 2}=0.00026$ H, $L_m = 0.012$ H, $R_1 = 0.03$ Ohm, $R'_2 = 0.03$ Ohm, $J = 1.5$ kgm².

The simulation results of the frequency startup of the IM drive using the 2nd-order AVIS method and other methods implemented in Matlab/Simulink for the used numerical integration step of 0.000002 s (corresponding to 10,000 points per period) are identical. These results

are considered to be the standard. Figures 3 to 7 present the standard waveforms of the frequency startup of the IM drive under nominal load. During the frequency startup, the stator voltage and its frequency linearly increase to the nominal value within 2 seconds (Fig. 2).

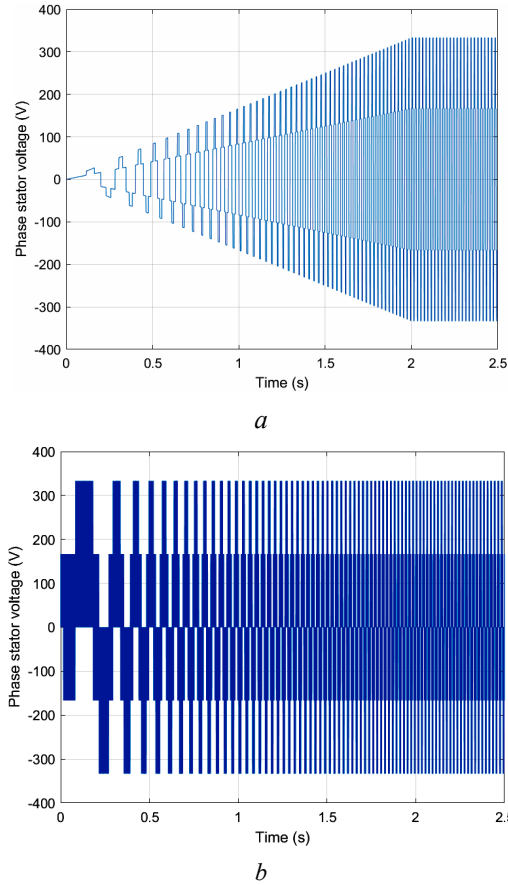


Fig. 2. Phase stator voltage of the IM supplied from (a) the six-step voltage source inverter and (b) from the PWM voltage source inverter.

At the same time, the peak value of the IM drive stator current during startup is three times higher than the nominal value (Fig. 3).

The peak value of the electromagnetic torque during startup does not exceed 2.5 times the nominal torque value (Fig. 4).

The increase in the rotation speed of the IM drive up to the nominal value occurs within 2 seconds (Fig. 5).

The adequacy of the developed model of the frequency-controlled electric drive, in the case of supplying the IM from a six-pulse voltage source inverter, has been confirmed by comparing the results of the physical experiment with the simulation results (Fig. 6).

The harmonic analysis of the IM stator current, in the case of its supply from a six-pulse voltage source inverter, indicates the presence of the 5th, 7th, 11th, 13th, and other higher harmonics in the stator current. The 5th and 7th harmonics have a significant influence on the current, with amplitudes of 37 % and 18 % of the fundamental harmonic, respectively.

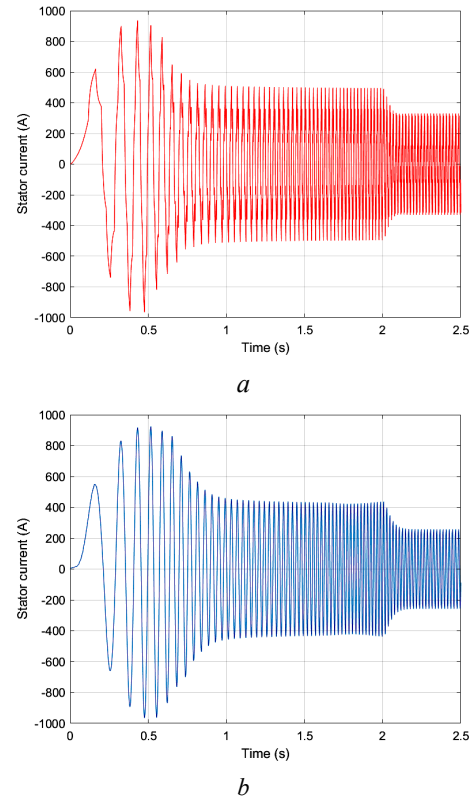


Fig. 3. Phase stator current of the IM supplied from (a) the six-step voltage source inverter and from (b) the PWM voltage source inverter

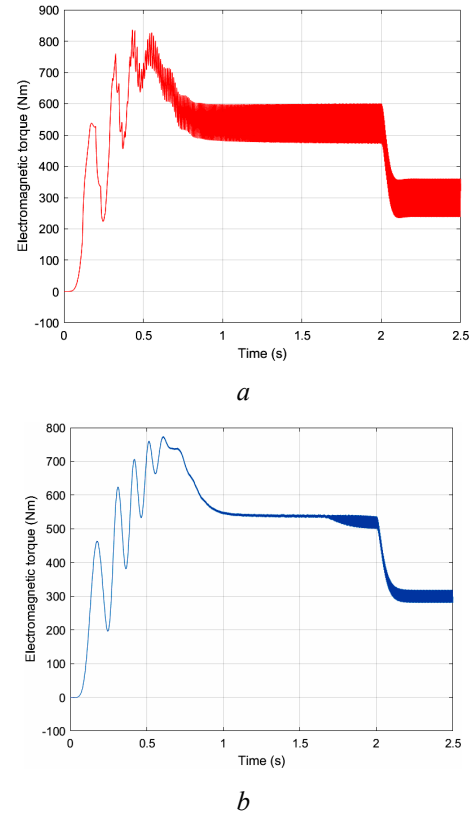


Fig. 4. Electromagnetic torque of the IM supplied from (a) the six-step voltage source inverter and (b) from the PWM voltage source inverter.

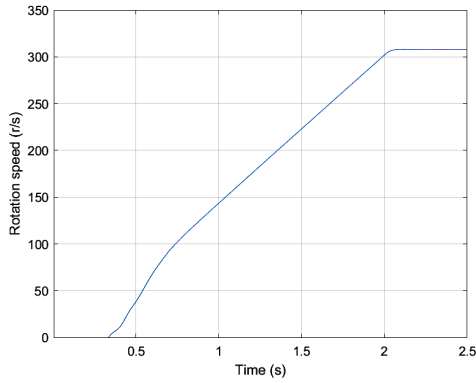
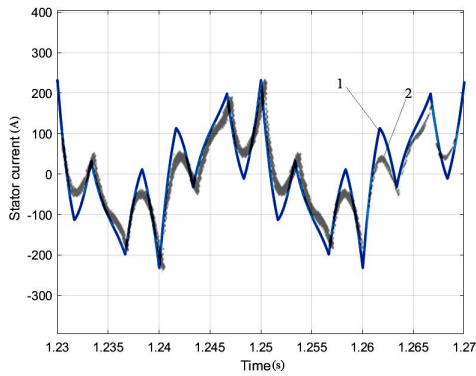
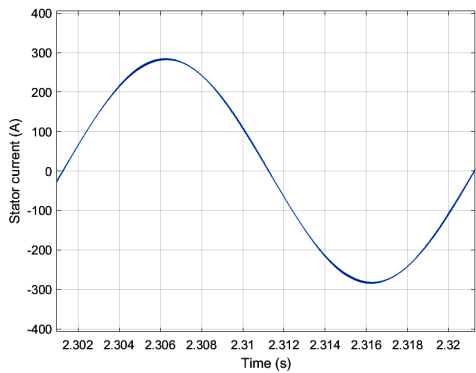


Fig. 5. Rotation speed of the IM.



a

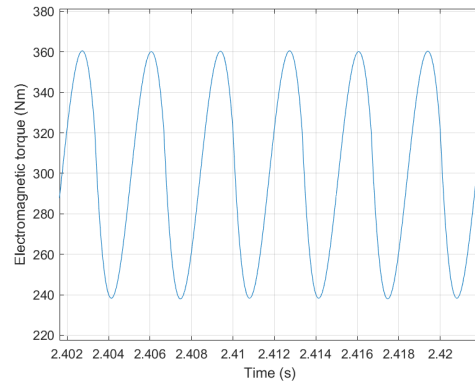


b

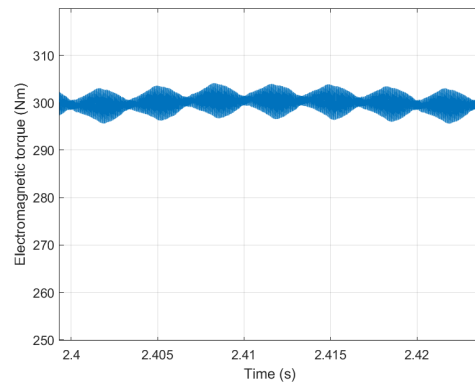
Fig. 6. Stator current of the IM supplied from (a) the six-step VSI and from (b) the PWM VSI in steady-state mode: simulation result (waveform 1) and experimental result (waveform 2) according to [1]

The electromagnetic torque of the IM in steady-state operation in the case of being supplied from six-step VSI produces ripples at a frequency of 300 Hz, with the amplitude of the pulsations being 40 % of the DC component of the torque (Fig. 7,a). The harmonic analysis of the IM electromagnetic torque in the case of being supplied from PWM VSI indicates the presence of the 6th, 12th, 18th, and other higher harmonics in the torque waveform. The 6th harmonic has a significant influence on the IM torque, with an amplitude of 20 % of the fundamental harmonic.

In the case of supplying the IM from PWM VSI, the amplitude of the torque pulsation is 3,3 % of the DC component (Fig. 7, b).



a



b

Fig. 7. Electromagnetic torque of the IM in the case of supplying it from the six-step VSI (a) and from the PWM VSI (b) in steady-state mode.

The input current of six-step VSI in steady-state operation exhibits pulsations at a frequency of 300 Hz, with the amplitude of the pulsations being 160 % of the DC component of the current (Fig. 8).

The harmonic analysis of the input current of six-step VSI (Fig. 8, a) indicates the presence of the 6th, 12th, 18th, 24th, and other higher harmonics in the input current waveform. The 6th and 12th harmonics have a significant influence on the input current of the inverter, with amplitudes of 43 % and 25 % of the fundamental harmonic, respectively.

When the numerical integration step is increased to 0.00002 (1,000 points per period) for the AVIS method and other known methods, an error compared to the reference solution occurs. Specifically, Figure 9 illustrates the electromagnetic torque of the IM obtained with the use of the 2nd-order AVIS method and the 4th-order Runge-Kutta method.

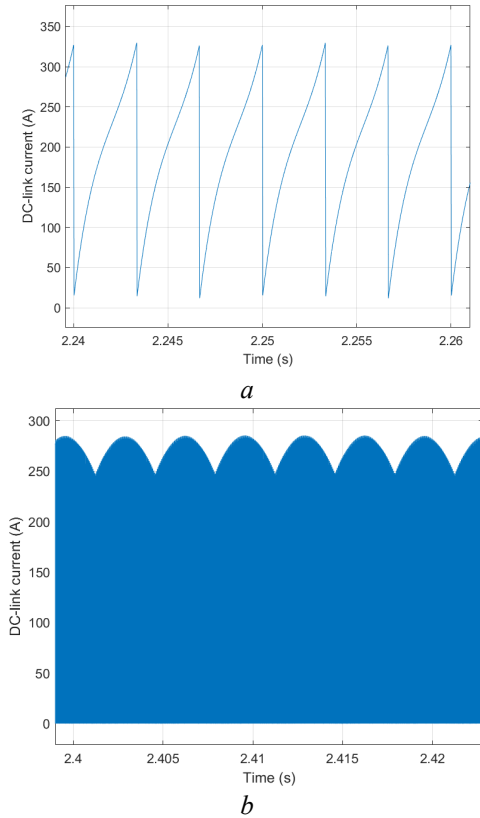


Fig. 8. Input current of the six-step VSI (a) and PWM VSI (b).

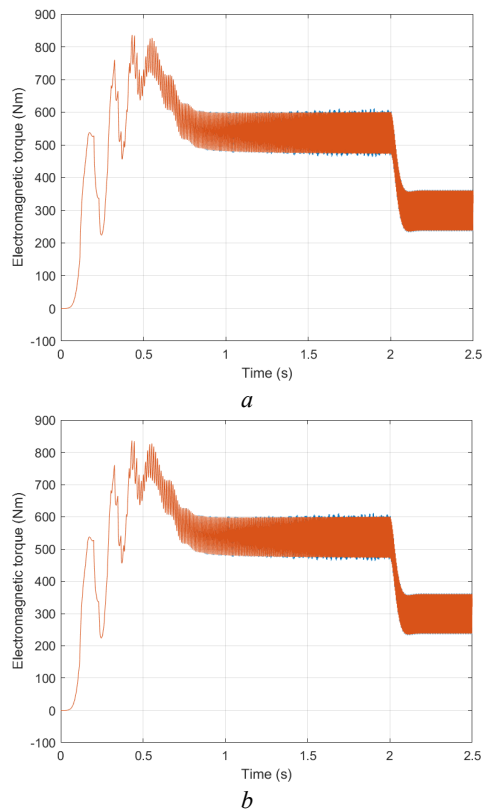


Fig. 9. Electromagnetic torque of the IM in the case of being supplied from six-step VSI for 1,000 points per period: a) 2nd-order AVIS method (blue waveform), b) the 4th-order Runge-Kutta method (blue waveform), standard (red waveform).

Increasing the numerical integration step (which corresponds to 100 points per period) leads to the increase in this error for all investigated methods of mathematical modeling (Fig. 10). The research has shown that this error is not caused by the calculation method itself, but rather by the incorrect reproduction of higher harmonics at small integration steps (loss of information due to the discretization of calculated curves, which is particularly evident in the higher harmonics of the current).

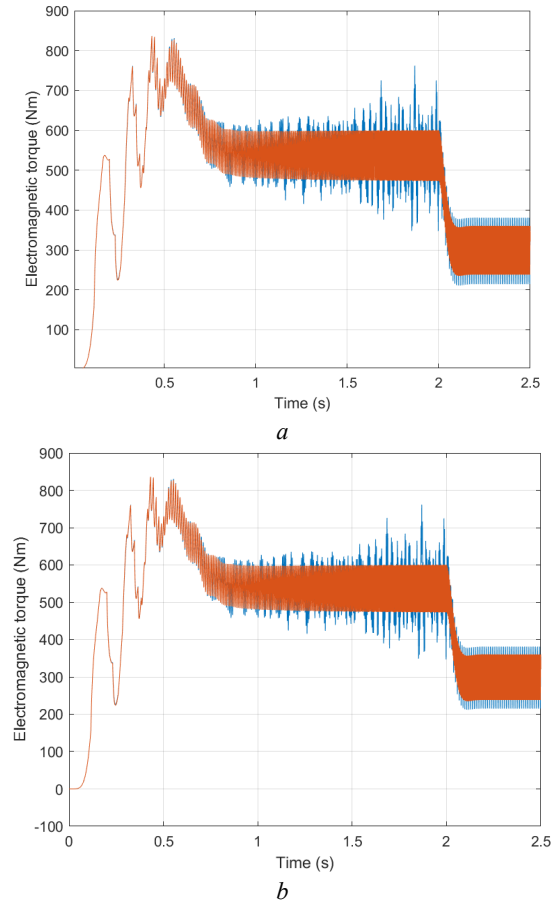


Fig. 10. Electromagnetic torque of the IM in the case of being supplied from six-step VSI for 100 points per period: a) 2nd-order AVIS method (blue waveform), b) the 4th-order Runge-Kutta method (blue waveform), standard (red waveform).

The second criterion by which the model effectiveness was evaluated was its computational speed of response. The computational speed of models implemented in the Matlab environment using methods such as AVIS 1, AVIS 2, Ode2, Ode3, Ode4, and Ode5 was compared. The results are presented in Table 1.

The comparison was conducted for a small step size, corresponding to 500,000 points per period, at which all methods showed equally accurate results. Therefore, the 1st and 2nd-order AVIS methods provide the best computational speed of response.

Table 1

**Speed of response for calculation time
of 2.5 sec corresponding to 500000 points**

Method	Calculation time, sec.
AVIS 1	15
AVIS 2	25
Ode2	43
Ode3	54
Ode4	62
Ode5	90

4. Conclusion

The mathematical model of a frequency-controlled induction electric drive created using the AVIS method is distinguished by increased calculation speed compared to traditional MATLAB models. The adequacy of the created model has been confirmed by comparing the obtained results with outcomes obtained through traditional MATLAB models, as well as by comparison with known results from physical experiments.

The created model operates in phase coordinates and enables conducting harmonic analysis of currents and electromagnetic torque of the induction motor, which is important for analyzing energy efficiency.

During mathematical modeling of frequency-controlled IM drives in phase coordinates, the numerical integration step should be determined on the basis of the required number of points per period to adequately capture the higher harmonics of currents. In this case, the reduction factor of the numerical integration step for modeling the IM drive with six-step VSI (compared to the sinusoidal supply) should correspond to the multiples of the most influential higher harmonics of the current, particularly the 5th and 7th harmonics.

References

- [1] M. A. Abbas, R. Christen and T. M. Jahns, "Six-Phase Voltage Source Inverter Driven Induction Motor", *IEEE Transactions on Industry Applications*, vol. IA-20, no. 5, pp. 1251-1259, 1984, doi: 10.1109/TIA.1984.4504591
- [2] G. Sieklucki, "An Investigation into the Induction Motor of Tesla Model S Vehicle", *2018 International Symposium on Electrical Machines (SME)*, 2018, pp. 1-6, doi: 10.1109/ISEM.2018.8442648.
- [3] D. W. Novotny, I. A. Lipo, *Vector control and dynamics of AC drives*, New York, Oxford University, 1996.
- [4] A. Kutsyk, A. Lozynskyy, V. Vantsevitch, O. Plakhtyna, L. Demkiv, "A Real-Time Model of Locomotion Module DTC Drive for Hardware-In-The-Loop Implementation", *Przegląd Elektro-techniczny*, vol. 97, pp. 60–65, 2021.
- [5] M. M. Kazachkovsky, *Autonomous converters and frequency converters*, Dnipro, Ukraine, 2000. (Ukrainian).

- [6] O. Plakhtyna, A. Kutsyk, and A. Lozynskyy, "Method of average voltages in integration step: Theory and application", *Electrical Engineering*, vol. 102(4), pp. 2413-2422. 2020.
- [7] O. Plakhtyna, A. Kutsyk, M. Semeniuk, "Real-Time Models of Electromechanical Power Systems, Based on the Method of Average Voltages in Integration Step and Their Computer Application", *Energies*, vol.13, p. 2263, 2020. <https://doi.org/10.3390/en13092263>
- [8] O. Kuznyetsov, "Mathematical model of a three-phase induction machine in a natural abc reference frame utilizing the method of numerical integration of average voltages at the integration step and its application to the analysis of electromechanical systems", *Mathematical Problems in Engineering*, vol. 2019, pp. 1–13, 2019, <https://doi.org/10.1155/2019/4581769>.
- [9] S. Cieřlik, "Mathematical Modeling of the Dynamics of Linear Electrical Systems with Parallel Calculations", *Energies*, vol. 14, p. 2930, 2021. <https://doi.org/10.3390/en14102930>.
- [10] Z. Kłowski, M. Fajfer, and Z. Ludwikowski, "Reduction of the Electromagnetic Torque Oscillation during the Direct on Line (DOL) Starting of a 6 kV Motor by Means of a Controlled Vacuum Circuit-Breaker", *Energies*, vol. 15, p. 4246, 2022. <https://doi.org/10.3390/en15124246>.

МАТЕМАТИЧНА МОДЕЛЬ ЧАСТОТНО-РЕГУЛЬОВАНОГО АСИНХРОННОГО ЕЛЕКТРОПРИВОДУ МЕТОДОМ СЕРЕДНІХ НАПРУГ НА КРОЦІ ЧИСЕЛЬНОГО ІНТЕГРУВАННЯ

Микола Семенюк, Андрій Куцик, Василь Тутка

Частотно-регульовані асинхронні електроприводи використовуються в різних галузях промисловості завдяки простоті та надійності конструкції електричної машини, а також здатності забезпечувати необхідні регульовальні характеристики. У статті наведено математичну модель частотно-регульованого електроприводу з інвертором напруги, розроблену методом середніх напруг на кроці чисельного інтегрування, та підтверджено її адекватність шляхом порівняння результатів математичного моделювання та фізичного експерименту. Порівняльний аналіз швидкодії та точності розрахунку моделі частотно-регульованого електроприводу методом середніх напруг на кроці чисельного інтегрування у порівнянні з відомими математичними моделями в Matlab/Simulink та відомими результатами фізичних експериментів продемонстрував ефективність використання методу середніх напруг для моделювання частотно-регульованих асинхронних електроприводів у фазних координатах з урахуванням реальних кривих струмів, потоку та електромагнітного моменту електронно-комутованих асинхронних машин.



Mykola Semeniuk graduated from Lviv Polytechnic National University and Mittelhessen University of Applied Sciences (Giessen, Germany). Currently, he is an Associate Professor at Lviv Polytechnic National University. His fields of interest are real-time mathematical modeling of electromechanical systems with multiwinding machines, control-system synthesis for power generation and power drive systems.



Vasyl Tutka received Mr. Sc. degree in electrical engineering in 2004 from the Ivano-Frankivsk National Technical University of Oil and Gas, he is an ingeneer at the PJSC Ivano-Frankivskcement (Ukraine). His research interests include modelling of electromechanical system and synthesis of their control.

Received: 24.05.2023, Accepted: 25.06.2023



Andriy Kutsyk received Dr. Sc. degree in electrical engineering in 2007 from Lviv Polytechnic National University. Currently, he is a Professor at Lviv Polytechnic National University (Ukraine). His research interests include real-time modelling of electromechanical system and synthesis of their control.